

JOINT PRIOR MODELS OF MUMFORD-SHAH REGULARIZATION FOR BLUR IDENTIFICATION AND SEGMENTATION IN VIDEO SEQUENCES

Hongwei Zheng and Olaf Hellwich

*Computer Vision & Remote Sensing, Berlin University of Technology
Franklinstrasse 28/29, Sekretariat FR 3-1, D-10587 Berlin*

Keywords: Bayesian estimation, point spread function, blind image deconvolution, Mumford-Shah functional, partial differential equations, Γ -convergence, piecewise smooth approximate, graph-grouping, segmentation.

Abstract: We study a regularized Mumford-Shah functional in the context of joint prior models for blur identification, blind image deconvolution and segmentation. For the ill-posed regularization problem, it is hard to find a good initial value for ensuring the soundness of the convergent value. A newly introduced prior solution space of point spread functions in a double regularized Bayesian estimation can satisfy such demands. The Mumford-Shah functional is formulated using Γ -convergence approximation and is minimized by projecting iterations onto an alternating minimization within Neumann conditions. The pre-estimated priors support the Mumford-Shah functional to decrease of the complexity of computation and improve the restoration results simultaneously. Moreover, segmentation of blurred objects is more difficult. A graph-theoretic approach is used to group edges which driven from the Mumford-Shah functional. Blurred objects with lower gradients and objects with stronger gradients are grouped separately. Numerical experiments show that the proposed algorithm is robust and efficiency in that it can handle images that are formed in different environments with different types and amounts of blur and noise.

1 INTRODUCTION

The challenge of blind image deconvolution (BID) is to uniquely define the optimized signals only from the degraded images. Segmentation of blur degraded images becomes more important. An ideal image f in the object plane is degraded by a linear space-invariant point spread function (PSF) h with an additive Gaussian white noise n using the linear degradation model $g = hf + n$. An observed image in the image plane g is formed by two unknown conditions h and n . The two-dimensional convolution is expressed as $hf = Hf = Fh$, where H and F are block-Toeplitz matrices and can be approximated by block-circulant matrices for large images. The point spread function (PSF) of blur is normally neither known nor perfectly known. Such blur identification can be considered as blind image deconvolution.

A regularization theory (Tikhonov and Arsenin, 1977) presents numerous challenges as well as opportunities for further statistical and mathematical vision modeling to solve ill-posed problems. This formalism has been recognized as a unified framework for studying several problems in early vision (Pog-

gio et al., 1985). However, the iterative Tikhonov regularization (Katsaggelos et al., 1991) and the total variation based regularization (Rudin et al., 1992) are mostly focused on the image restoration, denoising, or enhancement. A general regularization method proposed by Mumford and Shah (Mumford and Shah, 1989) has some natural advantages not only in image restoration but also in image segmentation. This functional has formulated restoration and segmentation problem mathematically in a energy minimization approach. Recently, the Mumford-Shah (MS) functional has been extensively explored for image segmentation and restoration (Aubert and Kornprobst, 2002). Through the literature study, most of these Mumford-Shah based methods are intensively tested on the influences of noises or occlusions but less experiments on the influences of blur. Blind image restoration and segmentation of degraded images are difficult but become more important in many vision systems. Combination of blur identification, image restoration and segmentation in the Mumford-Shah functional is a reasonable strategy for such tasks due to the mutual support of restoration and segmentation within a variational regularization. The reason is that accurate blur

identification and non-oversmoothing image restoration preserve more discontinuities and edges for accomplishing successful image segmentation. Furthermore, a variational regularization method expects to find the optimal solution efficiently and robustly based on some accurate prior information (Chan and Wong, 2000). The effective prior information and constraints are important to yield a unique solution to the corresponding optimization procedure.

The Bayesian estimation framework provides a structured way to include prior knowledge concerning the quantities to be estimated. The Bayesian approach is, in fact, the framework in which the most recent restoration methods have been introduced. Studies on existence, uniqueness, and stability of ill-posed early vision problems and related problems are investigated by Bertero, Poggio, and Torre (Bertero et al., 1988). Blake et al. (Blake and Zisserman, 1987) proposed the use of gradually non-convexity method, which can be extended to the blurring problem. Molina and Ripley (Molina and Ripley, 1989) proposed the use of a log-scale for the image model. Green (Green, 1990) and Bouman et al. (Bouman and Sauer, 1993) used convex potentials in order to ensure uniqueness of the solution. Recently, an appreciable extension of the range of hyperparameter estimation methods is used in Bayesian estimation. Molina et al. (Molina et al., 1999) used a hierarchical Bayesian paradigm resulting from the set theoretic regularization approach for estimating hyper-parameters. They also report that the accuracy of the obtained statistic estimates for the PSF and the image could vary significantly, depending on the initialization. To obtain accurate restorations in the Bayesian approach, accurate prior knowledge of PSF or image must be available.

In this paper, we investigate the Mumford-Shah regularization for image segmentation and restoration based on estimated PSF models. A newly introduced solution space of PSF priors supports accurate parametric PSF in the form of Bayesian MAP estimation. The PSF is estimated in a double L^2 norm regularized Bayesian estimation framework and is used to support the PSF value to the extended MS regularization. This makes some important effects: Firstly, it becomes possible to get good initial PSF value in Mumford-Shah regularization via a statistic method to decrease the complexity of computation. Secondly, it shows a theoretically sound way of how Mumford-Shah regularization can be processed for segmentation and restoration mutually. A graph cuts method is integrated to the Mumford-Shah functional for partitioning and grouping edges driven from the Mumford-Shah regularization. These edges are grouped using different strengths of gradients. The experimental results shows that this method yields encouraging results and is robust under different kinds and amounts of blur.

The paper is organized as follows. In Sect. (2), Bayesian estimation in the context of double regularizations for blur identification is described. In Sect. (3), the estimated PSFs support initial values for the Mumford-Shah regularization. A graph-theoretic concept is used to generate the result of segmentation. Experimental results are shown in Sect. (4). Conclusions are summarized in Sect. (5).

2 DOUBLE REGULARIZED BAYESIAN ESTIMATION

2.1 Bayesian Estimation with Joint Prior Solution Space of PSFs

The Bayesian MAP estimation utilizes a prior information to achieve a convergent posterior. Following a Bayesian paradigm, the true f , the PSF h and the observed g are formulated in

$$p(f, h|g) = \frac{p(g|f, h)p(f, h)}{p(g)} \propto p(g|f, h)p(f, h) \quad (1)$$

Applying the Bayesian paradigm to the blind deconvolution problem, we try to get convergence values from Eq. (1) with respect to f and h . This Bayesian MAP approach can also be seen as a regularization approach which combines optimization method for minimizing two proposed cost functions in the image domain and the PSF domain. The cost function of the restored true image f and PSF h from Eq. (1) are deducted respectively as the following,

$$\begin{aligned} L(f_{(g,h)}) &\propto p(g|f, h)p(f) \\ L(h_{(g,f)}) &\propto p(g|f, h)p_{\Theta}(h) \end{aligned} \quad (2)$$

For the application of these equations, some constraints of the PSF and the image are assumed due to the fact that the image pixels are independent identically distributed and does not influence the pixel correlations.

The proposed prior solution space supports the parametric structured PSFs in Bayesian estimation. We define a set Θ as a solution space of Bayesian estimation which consists of primary parametric blur models as $\Theta = \{h_i(\theta), i = 1, 2, 3, \dots, N\}$ and presented in Fig.(1). $h_i(\theta)$ represents the i th parametric model of the PSF with its defining parameters θ which denotes parameters of different PSFs in different manifolds, and N is the number of blur kernels.

$$h_i(\theta) = \begin{cases} h_1(\theta) \propto h(x, y; L_i, L_j) = 1/K, \\ \text{if } |i| \leq L_i \text{ and } |j| \leq L_j \\ h_2(\theta) \propto h(x, y) = K \exp(-\frac{x^2+y^2}{2\sigma^2}) \\ h_3(\theta) \propto h(x, y, d, \phi) = 1/d, \\ \text{if } \sqrt{x^2 + y^2} \leq D/2, \tan \phi = y/x \end{cases}$$

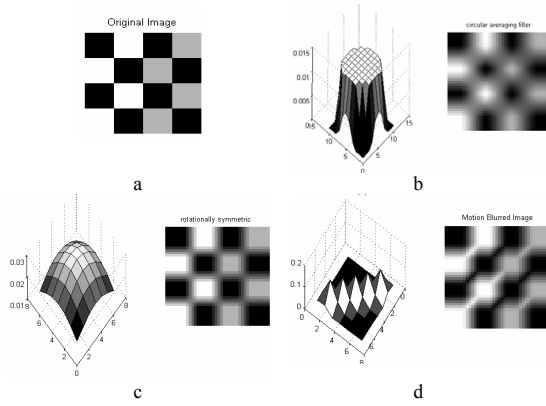


Figure 1: PSFs in the prior solution space. (a) Original synthetic image. (b) Pillbox PSF. (c) Gaussian PSF. (d) Linear motion PSF.

$h_1(\theta)$ is a Pillbox blur kernel with a length of radius K . $h_2(\theta)$ is a Gaussian PSF and can be characterized by parameters with its variance σ^2 and a normalized constant K . $h_3(\theta)$ is a simple linear motion blur PSF with a camera direction motion d and a motion angle ϕ . The other blur structures like out-of-focus and uniform 2D blur (Kundur and Hatzinakos, 1996) are also built in the solution space as *a priori* information. The prior solution space is constructed by a set of parametric PSFs for estimating unknown PSFs in the Bayesian MAP Estimation.

2.2 Estimation in the Image Domain and the PSF Domain

Based on the Tikhonov regularization, Lagendijk et al. (Lagendijk et al., 1988) made an extension of it by means of the theory of projections onto convex sets (POCS) (Katsaggelos et al., 1991) and the concepts of norms in a weighted Hilbert space. A weighted space-adaptive regularization equation then seeks to minimize the following cost function

$$\frac{1}{2} \sum_{x \in \Omega} w_1 (h(x) * f(x) - g(x))^2 + \frac{1}{2} \lambda \sum_{x \in \Omega} w_2 (c(x) * f(x))^2 = \min \quad (3)$$

where the cost function is minimized based on the degraded image $g(x)$, the ideal image $f(x)$, and the PSF $h(x)$. $c(x)$ is a regularization operator. $x \in \Omega$, $\Omega \subset R^2$ is the support size of a given image. λ is a regularization parameter that controls the trade-off between the fidelity to the observation and smoothness of the restored image. Weights w_1 and w_2 reduce these two effects adaptively to achieve better visual evaluation.

In the image domain, the cost function of image estimate can be minimized iteratively in the weighted

space-adaptive regularized formulation. In this equation, $p(g|f, h)$ follows a Gaussian distribution and $p(f)$ is a prior knowledge with some constraint conditions.

$$\begin{aligned} L(f_{(g,h)}) &= \arg \max_f [p(g|f, h)p(f)] \\ &= \frac{1}{2} \sum_{x \in \Omega} w_1 (g(x) - h(x) * f(x))^2 \\ &\quad + \frac{1}{2} \lambda \sum_{x \in \Omega} w_2 (c_1(x) * f(x))^2 \end{aligned} \quad (4)$$

where $p(f) \propto \exp \left\{ -\frac{1}{2} \lambda \sum_{x \in \Omega} w_2 (c_1(x) * f(x))^2 \right\}$, $p\left(\frac{g}{f,h}\right) \propto \exp \left\{ -\frac{1}{2} \sum_{x \in \Omega} w_1 (g(x) - h(x) * f(x))^2 \right\}$. Direct minimization of the cost function would lead to excessive noise magnification due to the ill conditioning of blur operator. A smoothness constraint $c_1(x)$ is a regularization operator and is usually a high-pass filter.

In the PSF domain, PSF can be seen as maximizing the conditional probability. However, manipulation of probability density functions (PDF) of PSFs in Bayesian estimation is difficult. A decision must be made firstly to attribute an accurate initial value in the regularization. The proposed prior solution space supports the parametric structured PSFs in Bayesian estimation. One more cost constraint of probability for the estimated PSF is then added in the equation. A new cost function for PSFs is following:

$$\begin{aligned} L(h_{(g,f)}) &= \arg \max_h \{p(g|h, f) p_{\Theta}(h)\} \\ &= \frac{1}{2} \sum_{x \in \Omega} w_1 (g(x) - h(x) * f(x))^2 \\ &\quad + \frac{1}{2} \beta \sum_{x \in \Omega} w_3 (c_2(x) * h(x))^2 \\ &\quad + \frac{1}{2} \gamma \sum_{x \in \Omega} w_4 |h - h_f|^2 \end{aligned} \quad (5)$$

Where $p_{\Theta}(h) \propto \frac{1}{2} \beta \sum_{x \in \Omega} w_3 (c_2(x) * h(x))^2 + \frac{1}{2} \gamma w_4 |h - h_f|^2$ is the prior knowledge and need to be computed firstly. h is a current estimated PSF and h_f is the final result of the estimated PSF for a given image. Since both ideal and observed image represent intensity distributions that cannot take negative values, the PSF coefficients are always nonnegative, $h(x) \geq 0$. Furthermore, since the image formation system normally does not absorb or generate energy, the PSF should satisfy $\sum_{x \in \Omega} h(x) = 1.0$. The probability of current PSF is computed in a Gaussian density function:

$$\begin{aligned} h_i(\theta^*) &= \arg \max_{\theta} p(h_i(\theta) | h) \\ &= \arg \max_{\theta} \log \left\{ (2\pi)^{-\frac{L*B}{2}} \left| \sum dd \right|^{-\frac{1}{2}} \right. \\ &\quad \left. * \exp \left[-\frac{1}{2} (h_i(\theta) - h)^T \sum dd^{-1} (h_i(\theta) - h) \right] \right\} \end{aligned}$$

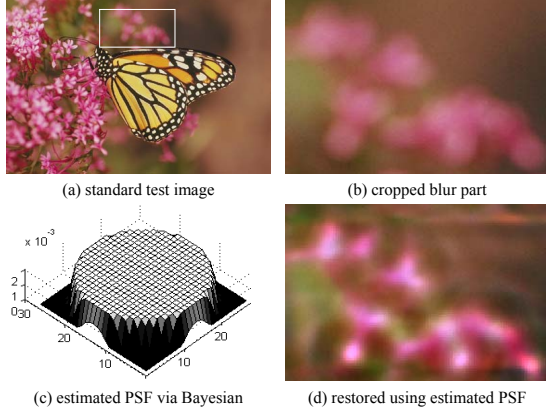


Figure 2: A estimated PSF using the prior solution space in the Bayesian MAP Framework.

We define the likelihood of the neighbor h and in resembling the i th parametric model $h_i(\theta)$, $h_i(\theta) \in \Theta$. The first subscript i denotes the index of the blur kernel. The modeling error $d = h_i(\theta) - h$ is assumed to be a zero-mean homogeneous Gaussian distributed white noise process with covariance matrix $\sum_{dd} = \sigma_d^2 I$ independent of $f(x, y)$. $L * B$ is an assumed support size of the blur kernel. The likelihood of the current PSF $l_{ij}(h)$ is computed using an Euclidean distance between the current PSF h and the corresponding probability model $h_i(\theta^*)$, $l_{ij}(h) = \sum_{i=1}^N \exp\{-|h_i(\theta^*) - h|^2 / [2tr(\sum_{dd})]\}$.

Motivated by the K-nearest neighbor concept, a weighted mean filter is used to determine the likelihood of h belonging to the i th parametric blur model. The mean value of likelihood $l_m(h)$ is $l_{ij}(h)$ weight-divided by $d(h, h_j)$. $d(h, h_j)$ is the Euclidean distance between h and its neighbor h_j . The weighted mean likelihood $l_m(h)$ should depend on two conditions. The first condition is the likelihood value of the blur manifold $l_{ij}(h)$, and the second is the distance between h and its neighbor PSF h_j . The final PSF h_f is obtained from the parametric PSF models using

$$h_f = \frac{[l_0(h)h + h_i(\theta^*) \sum_{m=1}^C l_m(h)]}{[\sum_{m=1}^C l_m(h)]}$$

where $l_0(h) = 1 - \max(l_m(h))$, $m = 1, \dots, C$. The optimal parametric model $h_i(\theta)$ is computed based on iterative estimated h . In reality, most blurs satisfy up to a certain degree of parametric structure. The main objective is to assess the relevance of current blur h with respect to parametric PSF models $h_i(\theta)$, and integrate these prior knowledge progressively into the computation scheme. If the current blur h is closely with the estimated PSF h_f , that means h belongs to a predefined parametric blur structure. Otherwise, if h differs from h_f significantly, it means that current blur h may not belong to the predefined PSF priors.

2.3 Alternating Minimization

To get an optimized PSF and image restoration, we use an alternating minimization (AM) approach. The AM decreases complexity. The cost functions of image and PSF are shown to be quadratic with positive semi-definite Hessian matrices. The two cost functions are convex functions which ensure convergence in the respective domains. The resulting method attempts to minimize double cost functions subject to some constraints such as non-negativity conditions of the image and energy preservation of PSFs. The objective of the convergence is to minimize double cost functions by combining these two cost equations. We propose to solve the equation as following:

$$\begin{aligned} \min_{h, f} L(f, h) &= \frac{1}{2} \sum_{x \in \Omega} w_1 (g(x) - h(x) * f(x))^2 \\ &+ \frac{1}{2} \lambda \sum_{x \in \Omega} w_2 (c_1(x) * f(x))^2 \\ &+ \frac{1}{2} \beta \sum_{x \in \Omega} w_3 (c_2(x) * h(x))^2 \\ &+ \frac{1}{2} \gamma \sum_{x \in \Omega} w_4 (h - h_f)^2 \end{aligned} \quad (6)$$

During the implementation, λ , β , γ including diagonal matrices assign different emphases based on the balance of the convergent PSF and image. The cost function of this equation is minimized in an AM approach via conjugate gradient descent with PSF prior (Zheng and Hellwich, 2006).

Derived from Eq. (6), we get two partial differential equations $p(x) = \partial L(f, h) / \partial f(x)$ and $q(x) = \partial L(f, h) / \partial h(x)$. The AM procedure is,

1. Initialization: $f^0(x) = g(x)$, $h^0(x)$ is an initial value. It is an estimated parametric PSF model h_f from the solution space.
2. n th iteration: $f_n(x) = \arg \min L_f(f | h_{n-1}, g)$, under a fixed $h(x)$.
3. $(n+1)$ th iteration: $h_{n+1} = \arg \min L_h(h | f_n, g)$, under a fixed $f(x)$, $h(x) \geq 0$.
4. If convergence is reached, then stop the iteration.

The global convergence of the algorithm to the local minima of cost functions can be established by noting the two steps 2 and 3. Since the convergence with respect to the PSF and the image are separated and optimized alternatively, the flexibility of this algorithm allows us to use conjugate gradient algorithm for computing the convergence. Conjugate gradient method utilizes the conjugate gradient direction instead of local gradient to search for the minima. Therefore, it is faster and also requires less memory storage when compared with quasi-Newton method. Fig. (2) shows a result of PSF estimation for a given image.

3 COUPLED SEGMENTATION AND BLIND RESTORATION

3.1 The Extended Γ -Convergence Mumford-Shah Regularization

When we get a estimated PSF for a given images, the PSF can be employed as an initial value for MS functional to decrease the complexity of computation and improve the optimization results. The basic idea of the MS functional is to subdivide an image into many meaningful regions (objects). It means to find a decomposition Ω_i of Ω and an optimal piecewise smooth approximation f given an observed image g . Thus, the estimated f varies smoothly within each Ω_i , and rapidly or discontinuously across the boundaries of Ω_i . It is also one kind of underlying connections with the graph-partitioning and grouping theory. The formula was considered as a minimization problem,

$$E(f, C) = \int_{\Omega} (f - g)^2 dx dy \quad (7)$$

$$+ \alpha \int_{\Omega \setminus C} |\nabla f|^2 dx dy + \beta |C|$$

where, $\Omega \subset R^2$ is a connected, bounded and open subset R^2 , f is the smoothed image $\subset \Omega \setminus C$, $g : \Omega \rightarrow R$ is a bounded image-function with uniform feature intensity, $C \subset \Omega$ is a finite set of segmenting curves and units of object boundaries, $|C|$ is the length of curve of C .

The task of this equation is to find f and Ω which minimize $E(f, C)$. The numerical minimization of the Mumford-Shah functional $E(f, C)$ is difficult due to the necessity to get the set C , keep track of possible changes of its topology, and calculate its length. Also, the number of possible discontinuity sets is enormous even on a small grid. Ambrosio and Tortorelli (Ambrosio and Tortorelli, 1990) applied a Γ -convergence to the Mumford-Shah functional which means to replace C by a continuous variable v . An irregular functional $E(f, C)$ is approximated by a sequence $E_{\varepsilon}(f)$ of regular functionals, $\lim_{\varepsilon \rightarrow 0} E_{\varepsilon}(f) = E(f, C)$ and the minimization of E_{ε} approximates the minimization of E . The edge set is represented by a characteristic function $(1 - x_C)$ which is approximated by an auxiliary function v of the gradient edge integration map, i.e., $v(x) \approx 0$ of $x \in C$ and $v(x) \approx 1$ otherwise. The functional thus becomes the form

$$E_{\varepsilon}(f, v) = \int_{\Omega} (f - g)^2 dx dy + \alpha \int_{\Omega} v^2 |\nabla f|^2 dx dy$$

$$+ \beta \int_{\Omega} \left(\varepsilon |\nabla v|^2 + \frac{(v - 1)^2}{4\varepsilon} \right) dx dy$$

We combine the image restoration and image segmentation based on MS functional using pre-estimated

PSFs. The generalized objective functional can be formulated in the following,

$$E_{\varepsilon}(f, h, v) = \int_{\Omega} (f * h - g)^2 dx dy \quad (8)$$

$$+ \alpha \int_{\Omega} v^2 |\nabla f|^2 dx dy$$

$$+ \beta \int_{\Omega} \left(\varepsilon |\nabla v|^2 + \frac{(v - 1)^2}{4\varepsilon} \right) dx dy$$

$$+ \gamma \int_{\Omega} |\nabla h|^2 dx dy$$

Different from the last equation, the first term uses the degradation model $h * f$ instead of f in the fidelity term. The last term represents the regularization of the blur kernel with its own variables which is estimated previously. This term is necessary to reduce the ambiguity in the division of the apparent blur between the recovered image and the blur kernels.

To minimize the cost of E_{ε} , the ideal image f , the edge integration map v and the PSF h are computed in an alternating minimization approach for getting an optimized value from their partial differential equation of E_{ε} . The minimization of this equation with respect to f and v is carried out based on Euler-Lagrange equations Eq. (9) and Eq. (10). The differentiation are

$$\frac{\partial E_{\varepsilon}}{\partial v} = 2\alpha v |\nabla f|^2 + \beta \left(\frac{v-1}{2\varepsilon} \right) - 2\varepsilon \beta \nabla^2 v \quad (9)$$

$$\frac{\partial E_{\varepsilon}}{\partial f} = (h * f - g) * h(-x, -y) - 2\alpha \text{Div}(v^2 \nabla f) \quad (10)$$

We can observe that Eq. (9) is a convex and lower bounded with respect to the functions f and v if the other one and the blur PSFs are estimated and fixed. ε is a small positive constants for discrete implementation. For solving these two equations, boundary conditions are need to be specified for the human perceptually demands and signal to noise ratio improvement (ISNR). The Neumann conditions $\partial E_{\varepsilon} / \partial v = 0$ and $\partial E_{\varepsilon} / \partial f = 0$ correspond to the reflection of the image across the boundary with the advantages of not imposing any value on the boundary and not creating edge on it. Given a blur degraded video sequence in Fig. (3)(b), we can observe that the gradient edge maps v are very different from the foreground blurred people to the unblurred cluttered background.

3.2 Coupled Segmentation Using Graph Cuts

To segment the blurred objects efficiently, we use the graph-theoretic segmentation method to group the edges driven from the Mumford-Shah functional. Shi and Malik (Shi and Malik, 2000) treated image segmentation as a graph partitioning and grouping problem using a global criterion for segmenting the graph.

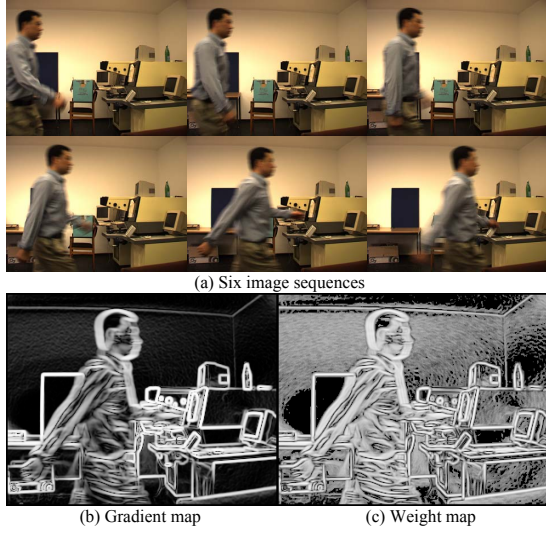


Figure 3: A walking man is blurred during the video recording period. Background objects are unblurred with stronger gradients edge map than the foreground people, produced by the proposed method.

The two partition criteria in the grouping algorithm is to minimize the disassociation between the groups and maximize the association within the group. The global criterion measures both the total dissimilarity between the different groups as well as the total similarity within the groups. This disassociation measure is called the normalized cut (Ncut): $Ncut(A, B) = \frac{cut(A, B)}{asso(A, V)} + \frac{cut(A, B)}{asso(A, V)}$. A and B are two disjoint sets, $A \cup B = V$, $A \cap B = \phi$. The Lanczos method is used to grouping similar objects which can speed up the running time.

We extend this idea to the Mumford-Shah functional for segmenting the blurred objects in video sequences. The reason is that the blurred objects and unblurred objects in a degraded image have different strength of gradients, i.e Fig. (3). The gradient edges in Fig. (3)(b) are computed using the extended Mumford-Shah regularization. The combination of low level processing and Mid or high level knowledge can be used to either confirm these groups or select some for further attention in repartitioning or grouping blurred and unblurred objects in images. The grouping algorithm is summarized as follows:

- Given a set of features, set up a undirected weight graph $G = (V, E)$, where V are the vertices and E are the edges between these vertices. V can correspond to pixels in an image or set of connected pixels. Computing the weight on each edge Fig. (3)(c), and summarize the information into W , and D .

- Solve $(D - W)x = \lambda Dx$ for eigenvectors with the smallest eigenvalues.

- Use the eigenvector with second smallest eigen-

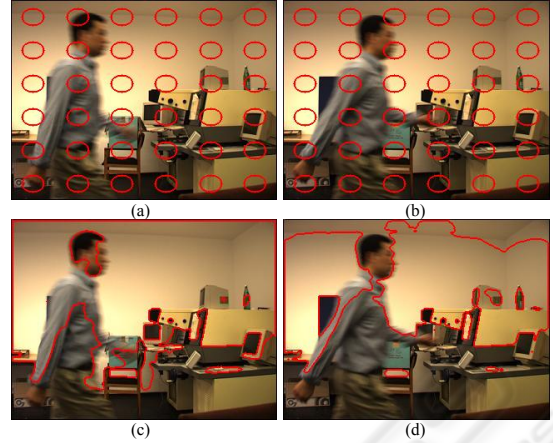


Figure 4: The result of segmentation for a blurred walking man using a Chan-Vese Method in two continuous images.

value to bipartition the graph by finding the splitting point such that $Ncut$ is maximized.

- Decide if the current partition should be subdivided by checking the stability of the cut, and make sure $Ncut$ is below pre-specified value.

- Recursively repartition the segmented parts if necessary. The number of groups segmented by this controlled by the maximum allowed $Ncut$.

4 NUMERICAL EXPERIMENTS

4.1 Discretisation

To solve the Γ -convergence to the MS functional, we use a discrete scheme called a cell-centered finite difference from (Vogel and Oman, 1998), (Weiser and Wheeler, 1988). Following the way of discretization, Eq. (9) is written in a discrete form,

$$2\alpha v_{ij} [(\Delta_+^x f_{ij})^2 + (\Delta_+^y f_{ij})^2] + \beta \cdot \frac{v_{ij} - 1}{2\varepsilon} \quad (11)$$

$$- 2\beta\varepsilon (\Delta_+^x \Delta_-^x v_{ij} + \Delta_+^y \Delta_-^y v_{ij}) = 0$$

where the forward and backward finite difference approximations of the derivatives $\partial f(x, y)/\partial x$ and $\partial f(x, y)/\partial y$ and denoted by $\Delta_\pm^x f_{ij} = \pm(f_{i\pm 1, j} - f_{ij})$ and $\Delta_\pm^y f_{ij} = \pm(f_{i, j\pm 1} - f_{ij})$. To minimize the column-stack ordering of $\{v_{ij}\}$, the system is of form $Mv = q$, where M is symmetric and sparse matrix and solve the minimization using Minimal residual algorithm. Let H denote the operator of convolution of different blur PSFs that are pre-estimated. Using the notation of (Vogel and Oman, 1998), let $L(v)$ denote the differential operator $L(v)f = -Div(v^2 \nabla f)$. Eq. (10) can be expressed as $H^*(Hu - g) + 2\lambda L(v)f = 0$. Let $A(v)f = H^*f +$

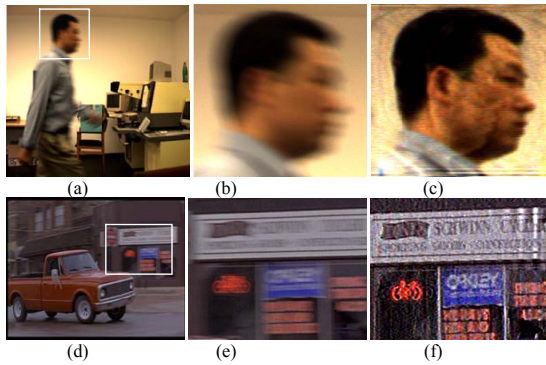


Figure 5: Blind deconvolution of degraded objects in video sequences using estimated PSFs. (a)(d) Real video frames. (b)(e) Blurred parts in video. (c)(f) Results of blind deconvolution using the weighted L^2 norm regularization.

$2\lambda L(v)f$, we get $A(v)f = H^*g$. f is iteratively determined. To obtain f^{n+1} , a correction term d^n is added to the current value f^n : $f^{n+1} = f^n + d^n \times d^n$ is estimated by $A(v)d^n = H^*g - A(v)f^n$ via the convergent descent method. Gradient edges and the restored image are computed.

4.2 Results and Discussions

Experiments on simulated data and real data are carried out to demonstrate the effectiveness of our algorithm. The advantage of our method is that the discontinuity set is not isolated closed contours. For such cluttered images in Fig. (4), some of closed contour curves using curve evolution technique (Chan and Vese, 2001), are removed due to some boundary leaks, stronger gradient differences, etc.

In this experiment shown in Fig. (5), we illustrate the capability of the proposed algorithm to handle real-life video data degraded by non-standard blur. The video frames are captured from films or video data with unknown shapes and sizes of the actual blur. The degraded images are separated into RGB colour channels and each channel is processed accordingly. Based on the estimated PSFs and parameters in the L^2 norm regularization approach, the accurate PSF model helps to get the results. We also compare the blind deconvolution results generated from the weighted L^2 norm regularization and the Mumford-Shah restoration. The parameters in the Mumford-Shah functional are tuned for the best performance $\alpha = 10^{-4}$, $\beta = 10^{-8}$, $\varepsilon = 10^{-3}$ with an previously estimated PSF from regularized Bayesian estimation. The value of ε and β can be increased in the presence of noise. From the results, we can found that the Mumford-Shah functional is sharper than the L^2 norm regularization approach using the same estimated PSF shown in Fig. (6). It highlights the ad-

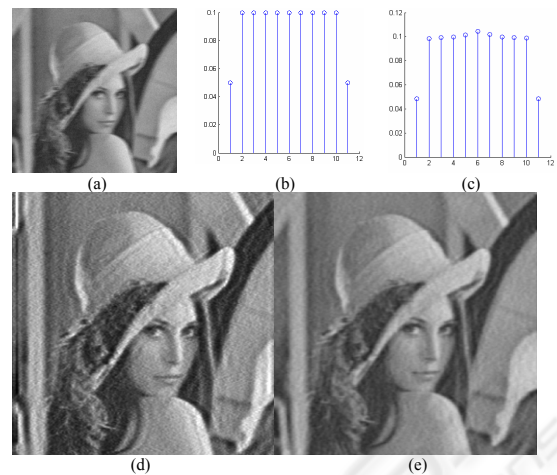


Figure 6: Blind restored Images from L^2 norm and MS functional. (a) Motion blur with 20 dB Gaussian noisy image. (b) The original PSF. (c) The estimated PSF in 2D. (d) The L^2 norm restored image using the estimated PSF. (e) The Mumford-Shah restored image using the estimated PSF.

vantage of the MS functional than the weighted L^2 regularization.

The third experiment is performed using the suggested method. Segmentation of a video sequences has good performance shown in Fig. (7). Cluttered background objects with stronger gradients do not influence the segmentation of blurred objects with lower gradients. The PSF is firstly blur identified. The estimated PSF directly supports the Mumford-Shah based segmentation to improve the accuracy of edge detection. For the given video sequences, the PSF is identified as a stronger motion blur. v is firstly initialized as 1, the edges with some gradients are computed after a few iterations in the extended Mumford-Shah regularization. These detected edges are grouped via the *Ncuts* method into numerical groups. The result is labeled following the grouped regions. From the Fig. (7), we can observe that the blurred walking man is accurately segmented.

5 CONCLUSIONS

The paper presents a Mumford-Shah based regularization using estimated PSFs prior. Blind image deconvolution is one kind of ill-posed inverse problem. Searching for the solution in the largest space is not a good strategy. A prior knowledge should be used from different viewpoints to improve the solution. Support of accurate prior information directly to the computation is an excellent strategy since the approach improves the accuracy of initial value. Using the PSF prior, the Mumford-Shah functional is then

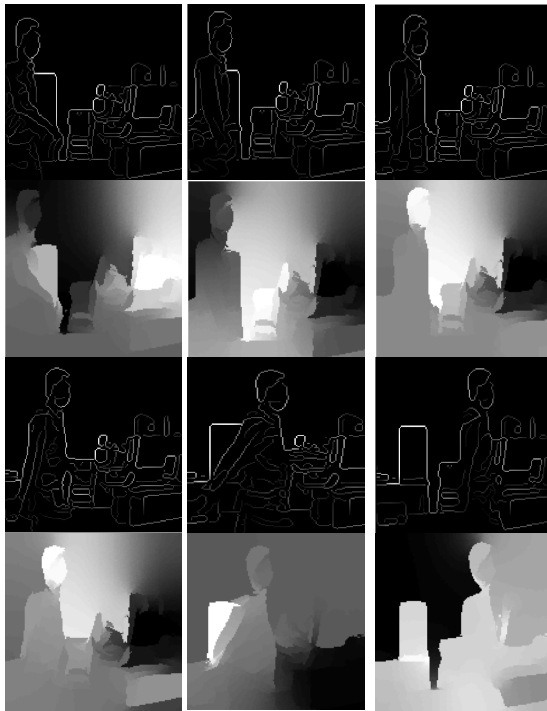


Figure 7: The results of segmentation for a blurred walking man using the MS functional and the graph-grouping method in six continuous images.

simplified into two partial differential equations for the image and edges and becomes more robust for different types of blur. During the image segmentation, graph theory is integrated to partition and group the edges driven from the Mumford-Shah functional. These lower gradient blurred objects can then be segmented accurately without any prior knowledge. It is clear that the proposed method is instrumental in blind image deconvolution and segmentation and can be easily extended in practical environments.

REFERENCES

Ambrosio, L. and Tortorelli, V. M. (1990). Approximation of functionals depending on jumps by elliptic functionals via γ -convergence. *Communications on Pure and Applied Mathematics*, 43:999–1036.

Aubert, I. and Kornprobst, P. (2002). *Mathematical problems in image processing: partial differential equations and the Calculus of Variations*. Springer.

Bertero, M., Poggio, T. A., and Torre, V. (1988). Ill-posed problems in early vision. *Proceedings of the IEEE*, 76(8):869–889.

Blake, A. and Zisserman, A. (1987). *Visual Reconstruction*. MIT Press, Cambridge.

Bouman, C. and Sauer, K. (1993). A generalized gaussian image model for edge-preserving map estimation. *IEEE Transactions of Image Processing*, 2:296–310.

Chan, T. F. and Vese, L. A. (2001). Active contours without edges. *IEEE Trans. on Image Processing*, 10(2):266–277.

Chan, T. F. and Wong, C. K. (2000). Convergence of the alternating minimization algorithm for blind deconvolution. *Linear Algebra Appl.*, 316:259–285.

Green, P. (1990). Bayesian reconstruction from emission tomography data using a modified em algorithm. *IEEE Tr. Med. Imaging*, 9:84–92.

Katsaggelos, A., Biemond, J., Schafer, R., and Mersereau, R. (1991). A regularized iterative image restoration algorithm. *IEEE Tr. on Signal Processing*, 39:914–929.

Kundur, D. and Hatzinakos, D. (1996). Blind image deconvolution. *IEEE Signal Process. Mag.*, May(5):43–64.

Legendijk, R., Biemond, J., and Boeke, D. (1988). Regularized iterative image restoration with ringing reduction. *IEEE Tr. on Ac., Sp., and Sig. Proc.*, 36(12):1874–1888.

Molina, R., Katsaggelos, A., and Mateos, J. (1999). Bayesian and regularization methods for hyperparameters estimate in image restoration. *IEEE Tr. on S.P.*, 8.

Molina, R. and Ripley, B. (1989). Using spatial models as priors in astronomical image analysis. *J. App. Stat.*, 16:193–206.

Mumford, D. and Shah, J. (1989). Optimal approximations by piecewise smooth functions and associated variational problems. *Communications on Pure and Applied Mathematics*, 42:577–684.

Poggio, T., Torre, V., and Koch, C. (1985). Computational vision and regularization theory. *Nature*, 317:314–319.

Rudin, L., Osher, S., and Fatemi, E. (1992). Nonlinear total variation based noise removal algorithm. *Physica D*, 60:259–268.

Shi, J. and Malik, J. (2000). Normalized cuts and image segmentation. *IEEE Transactions on Pattern Analysis and Machine Intelligence*, Aug.:888–905.

Tikhonov, A. and Arsenin, V. (1977). *Solution of Ill-Posed Problems*. Wiley, Winston.

Vogel, R. V. and Oman, M. E. (1998). Fast, robust total variation-based reconstruction of noisy, blurred images. *IEEE Trans. on Image Processing*, 7:813–824.

Weiser, A. and Wheeler, M. F. (1988). On convergence of block-centered finite differences for elliptic problems. *SIAM J. Numer. Anal.*, 25:351–275.

Zheng, H. and Hellwich, O. (2006). Double regularized bayesian estimation for blur identification in video sequences. *In LNCS of Asian Conference on Computer Vision, ACCV06*, pages 943–952.